

# Combining Artificial Intelligence and Image Processing for Diagnosing Diabetic Retinopathy in Retinal Fundus Images

<https://doi.org/10.3991/ijoe.v18i13.33985>

Obaida M. Al-hazaimeh<sup>1</sup>(✉), Ashraf A. Abu-Ein<sup>1</sup>, Nedal M. Tahat<sup>2</sup>,  
Ma'moun A. Al-Smadi<sup>1</sup>, Malek M. Al-Nawashi<sup>1</sup>

<sup>1</sup>Al-Balqa Applied University, Irbid, Jordan

<sup>2</sup>The Hashemite University, Zarqa, Jordan

dr\_obaida@bau.edu.jo

**Abstract**—Retinopathy is an eye disease caused by diabetes, and early detection and treatment can potentially reduce the risk of blindness in diabetic retinopathy sufferers. Using retinal Fundus images, diabetic retinopathy can be diagnosed, recognized, and treated. In the current state of the art, sensitivity and specificity are lacking. However, there are still a number of problems to be solved in state-of-the-art techniques like performance, accuracy, and being able to identify DR disease effectively with greater accuracy. In this paper, we have developed a new approach based on a combination of image processing and artificial intelligence that will meet the performance criteria for the detection of disease-causing diabetes retinopathy in Fundus images. Automatic detection of diabetic retinopathy has been proposed and has been carried out in several stages. The analysis was carried out in MATLAB using software-based simulation, and the results were then compared with those of expert ophthalmologists to verify their accuracy. Different types of diabetic retinopathy are represented in the experimental evaluation, including exudates, micro-aneurysms, and retinal hemorrhages. The detection accuracies shown by the experiments are greater than 98.80 percent.

**Keywords**—diabetic retinopathy, machine learning, deep learning, Fundusimages, ophthalmology, object detection, DCNN, object classification

## 1 Introduction

Nowadays, retinal inflections are an important part of the diagnosis of diabetic retinopathy, and a Fundus image is essential. Nearly 347 million people are visually impaired, according to the World Health Organization's projections for 2010. Using automatic approach for detecting and classifying retinal diseases, blindness has been reduced significantly in recent years [1, 2]. Early detection of Diabetic Retinopathy is the most effective treatment for this disease [3]. As a general rule, diabetic retinopathy stages are broken down into four levels of severity as shown in Figure 1. Exudates, retinal

hemorrhage and micro-aneurysms need to be identified and studied to detect the early stage of diabetic retinopathy [2, 4].

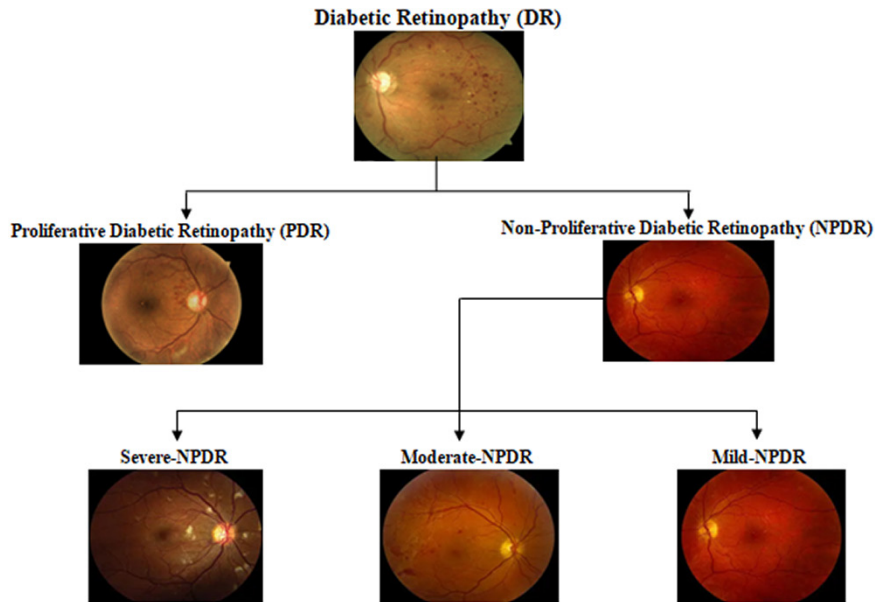


Fig. 1. Diabetic retinopathy stages

Detection and analysis of diabetic retinopathy can benefit from the use of an automated feature extraction process [5]. Preventable features in retinal images should be avoided robustly and automatically as a result of the early detection and treatment of these diseases. Figure 2 depicts the retina's features [6].

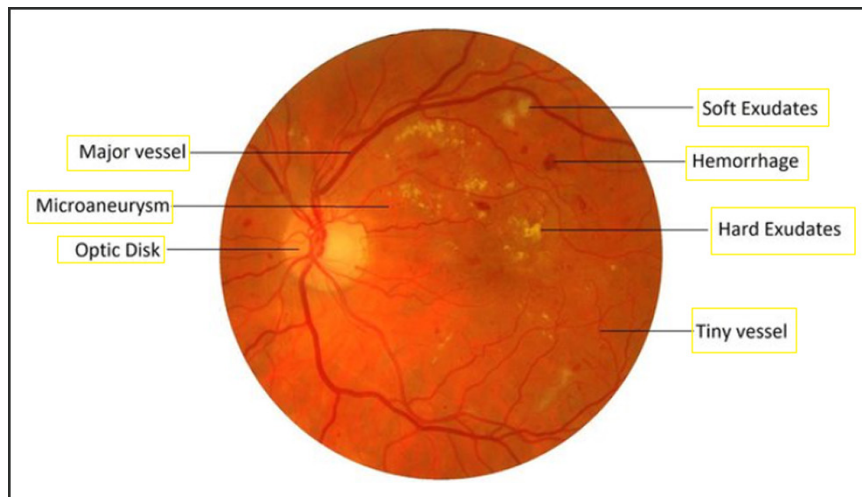


Fig. 2. Features of interest in a retinal fundus image

Diabetes retinopathy, or damage to the retina caused by diabetes, is known as a silent disease because it only becomes apparent when the condition has progressed to this point. There is a correlation between the onset of diabetes and the duration of the disease [7, 8]. Contrast enhancement, noise removal, color space selection, and color normalization are all used to detect exudates automatically [9]. Optic disc localization and segmentation are both critical components in the exudates detection. Ophthalmologists could benefit from this method because it can detect diabetic retinopathy symptoms quickly and easily. In order to improve performance, some pre-processing stages of the decision tree and GA-CFS could be used to detect exudates automatically [2]. The non-exudates pixel level is detected by identifying significant features. Diabetic Retinopathy has three main diseases that can be difficult to detect (i.e., retinal hemorrhage, exudates, and micro-aneurysm). As a result, this paper proposed a new approach for the detection of diabetic retinopathy disease from retinal Fundus images. Noise reduction, feature extraction, features selection, and diagnosis of diabetic retinal diseases are the four phases in the proposed method.

The following is the structure of the paper: Section (2) examines publications that are related to our proposed approach and discusses in depth how our approach advances the state-of-the-art. Section (3) goes into great detail on the proposed approach. Section (4) provides the output produced experimental results as well as pertinent discussions concerning the performance of the proposed work and a comparison with state-of-the-art approaches. Section (5) summarizes and discusses the results.

## **2 Related work**

An early diagnosis of retinal disease can be made using images of the retinal Fundus. Image processing algorithms can detect and identify diabetic retinopathy diseases [3]. Here, we'll take a look at some of the most cutting-edge approaches in use today. Exudates, blood vessels, and micro-aneurysms were all included in a new classification system developed by Paing et al. [10]. An artificial neural network was used to classify the retinal diseases, as well as grade and stage them, using Fundus images. Using retinal Fundus images, M. Purandare and K. Noronha [11] introduced a hybrid approach for automatically detecting and classifying retinal lesions and diabetic retinopathy. According to the study, features such as a non-segmented texture, blood vessel, and area exudates area were extracted. The SVM classifier was used for feature vector classification. In order to detect diabetic retinopathy, Zhou et al. [12] used a deep multiple instance learning (i.e., MIL) technique to identify DR and lesions in retinal Fundus images. Fundus images were processed using a Convolutional Neural Network (i.e., CNN) and to classify lesions and DR the global aggregation was used. Suriyal et al. [13] created a mobile app that uses deep learning to identify DR in real time for diabetic patients. Based on tensor flow DNN architecture, this application was trained and tested on Fundus images. Gulshan et al. [14] used deep learning to develop a DR detection method based on Fundus images. For retinal image analysis, the optimized model utilized two datasets: EyePACS-1 and Messidor-2, both of which were trained using a deep convolutional neural network. Gondal et al. [15] introduced a methodology for the detection of retinal degenerative disease (DR) lesions in the Fundus images. A convolutional

neural network was used to identify DR lesions in Fundus images using the developed technique. In experiments and performance evaluations, the DiaretDB1 dataset was used and achieved 95.4 percent accuracy in detecting DR lesions. A significant algorithm was developed by Faust et al. [16] for detecting diabetic retinopathy. Different algorithms were used to extract the features from digital retinal Fundus images. Table 1 summarizes the most relevant research in the field of diabetic retinopathy detection.

**Table 1.** Most relevant research study – state-of-the-art methods – comparison

Ref. No.	Method	Dataset	Performance Evaluation	Year
			Accuracy	
[17]	CNNs	E-Ophtha, DIARETDB1	98.00%	2019
[18]	Random Forest Classifier	DIARETDB0, DIARETDB1.	93.58%	2019
[19]	Dynamic Decision Thresholding	STARE, E-Ophtha Ex, DIARETDB1, MESSIDOR.	93.46%	2018
[20]	Deep CNN	EyePACS.	82.00%	2018
[21]	CNNs	D1.	98.27%	2016
[22]	Region based Multiscale LBP Texture Approach	DIARETDB0.	96.73%	2016
[23]	Fuzzy Techniques	STARE, DIARETDB0, DIARETDB1, MESSIDOR.	93.00%	2016
[24]	Adaptive Histogram Equalization, Iterative Thresholding Approach	Gaziosmanpasa University	94.10%	2019
[25]	Adaptive Histogram Equalization, Background Estimation	DIARETDB1.	95.42%	2019
[13]	DCNN	KAGGLE.	73.30%	2018
[10]	Artificial Neural Network	MESSIDOR, KAGGLE.	96.00%	2016
[26]	Multiclass Discriminate Analysis	RealDS	90.90%	2015
[27]	Morphological Operations and Segmentation	DIARETDB1	97.75%	2015
[28]	VGG-19	KAGGLE	98.34%	2018
[29]	Deep Re-current Architecture	DIARETDB0, DIARETDB1, MESSIDOR.	90.00%	2017
[11]	Hybrid System	DOKMCM	92.00%	2016
[30]	R-sGAN Technique	DRIVE, STARE, HRF, IOSTAR	96.46%	2018
[31]	CHT, Localized Active Contour Model	RIM-ONE	98.00%	2019
[32]	Graph Machine Learning	Car1 Zeiss	86.00%	2015
[33]	The Existing Super Classification	ORIGA	85.00%	2021

### 3 Proposed approach

Using retinal Fundus images, this paper proposes a new method for detecting diabetic retinopathy diseases such as exudates, micro-aneurysms, and retinal hemorrhages. An overview of our proposed approach for detecting diabetic eye disease architecture's block diagram is shown in Figure 3. Our approach's implementation is discussed in detail in this section.

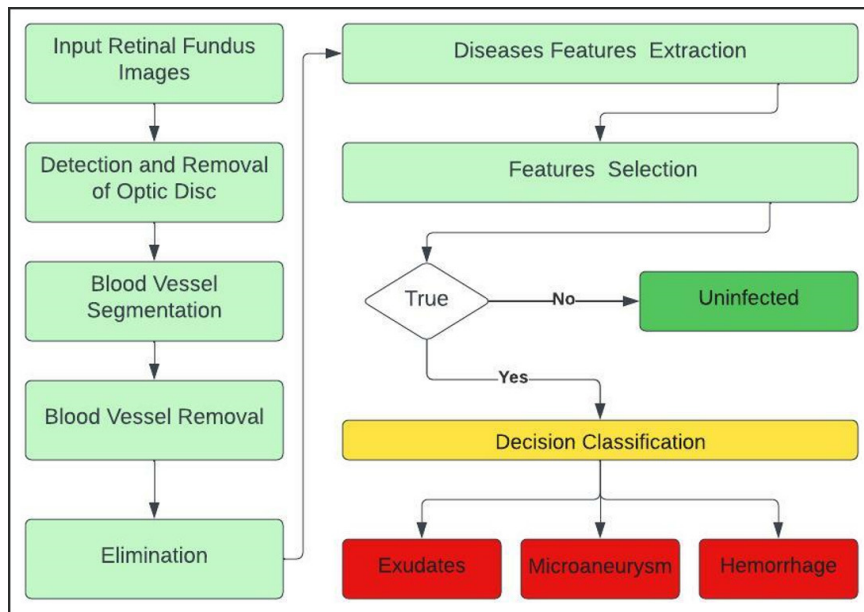


Fig. 3. Diagram of the proposed approach

#### 3.1 Pre-processing

In most image processing concepts, pre-processing is a vital part of the process. *HSI* conversion, *DE* noising, and other pre-processing steps take place during this stage [34–36]. In image processing, *HSI* conversion is useful because it displays colors as the human eye perceives them. Each color has three components (i.e., hue (*H*), saturation (*S*), and intensity (*I*)). Figure 4 shows the *HIS* color conversion [35].

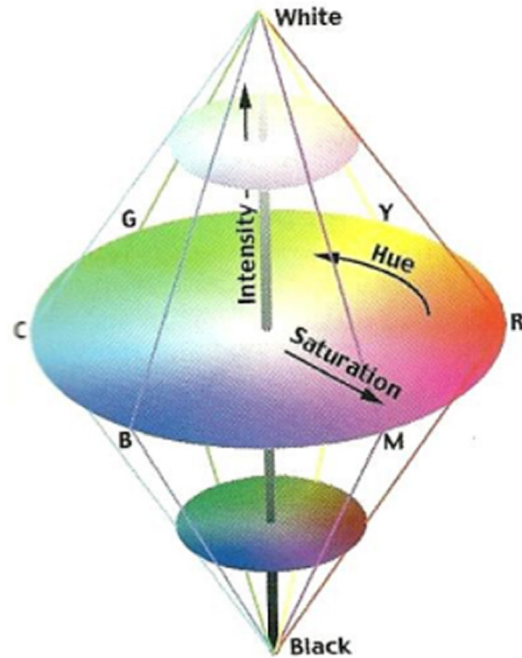


Fig. 4. HIS model conversion

Typically, retinal Fundus images submitted by ophthalmologists in public databases will be displayed in *RGB* format. *HSI* can be created from this *RGB* format as shown in Figure 5. In order to obtain an *HSI*, The formulas used are [35]:

$$Saturation (S) = 1 - \frac{3}{(R + G + B)} \min(R, G, B), \quad (1)$$

$$Intensity (I) = \frac{1}{3}(R + G + B)$$

If  $B \leq G$

$$Hue(H) = \cos^{-1} \left\{ \frac{0.5(R - G) + (R - B)}{(R - G)^2 + (R - G)(G - B)^{\frac{1}{2}}} \right\},$$

Else,  $H = 360 - H$

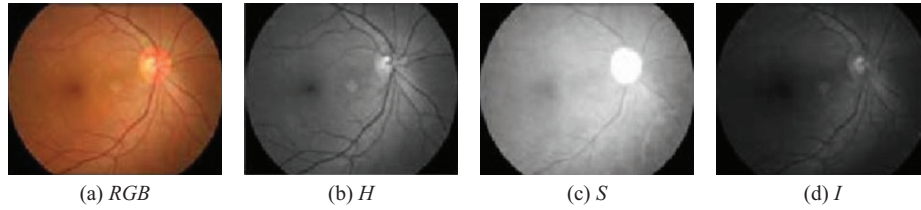


Fig. 5. HSI conversion

Because all images taken from databases contain noises during image collecting, coding, processing, and transmission, DE noising is highly crucial before image processing stage [2, 3]. Non-linear wiener filter with quad tree decomposition removes noise. CLAHE (“Contrast Limited Adaptive Histogram Equalization”) must be applied after the DE noising procedure has been completed to make the lighting more even. Retinal images can be improved by utilizing the CLAHE method to boost contrast [37] as shown in Figure 6. Remove noise from a retinal Fundus image by:

$$f(g) = \frac{1}{\sigma^2 \sqrt{2\pi}} e^{-\frac{(g-m)^2}{2\sigma^2}} \quad (2)$$

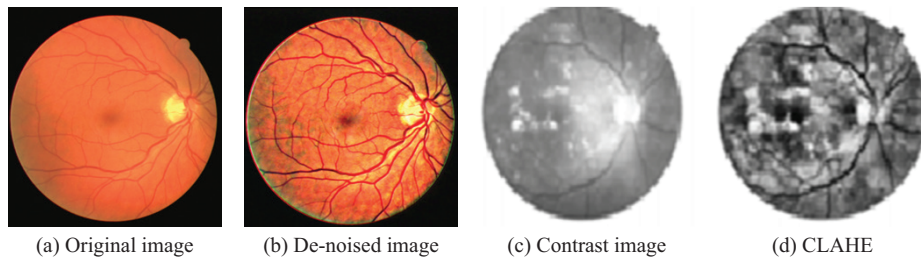


Fig. 6. Results of the pre-processing phase

### 3.2 Optic disc-based detection and removal

This phase is crucial in order to detect exudates since the left and right eyes may be able to recognize patterns that are similar in appearance. In order to efficiently detect exudates, we must detect and remove the Optic disc in this paper. The proposed method uses CHT (i.e., Circular Hough Transform) for the detection of optical discs. An image’s shape may always be determined using the CHT approach. This is the main advantage of the CHT approach, which is tolerant of feature border gaps and is not influenced by image noise [38]. An explanation of the circular Hough Transform concept can be found in Figure 7 [38]. Figure 8 shows the results of intermediate processing for Optic disc localization and removal. The Hough transform is based on the circle equation, expressed as:

$$(x_i - a)^2 + (y_i - b)^2 = r^2 \quad (3)$$

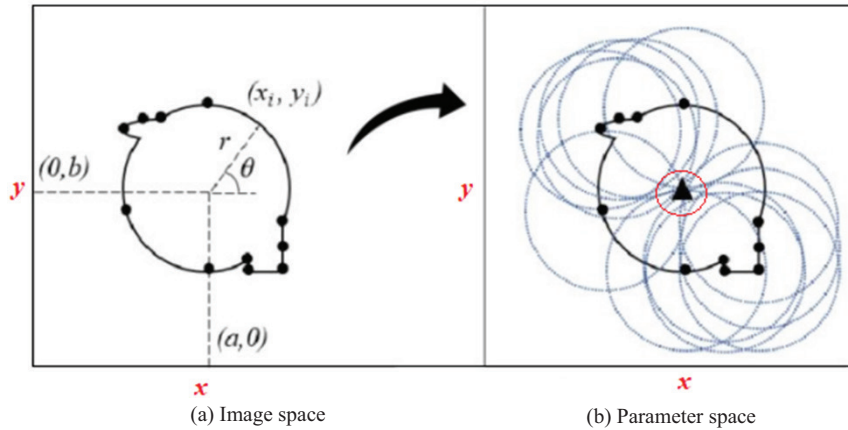


Fig. 7. Concept of the Circular Hough Transform

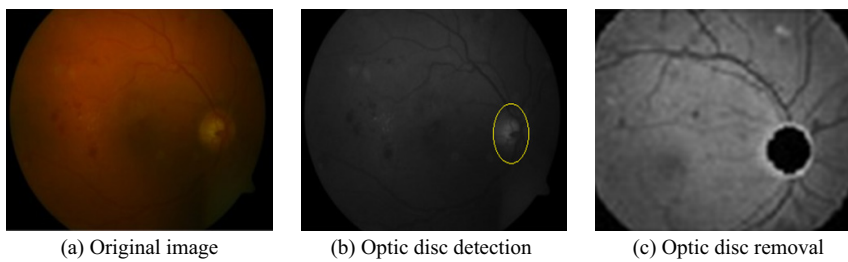


Fig. 8. Optic disc-detection and removal

### 3.3 Blood vessel-based segmentation and removal

It is common practice to locate the optic nerve, the fovea, and lesions using blood vessels as landmarks. The color, tortuosity, and diameter of the blood vessels are all likely to be abnormally high. Blood vessels have previously been distinguished from other characteristics by using a variety of attributes [39]. To accurately segment the blood vessels, plenty of segmentation techniques were applied. There is no spatial information added to the retinal images using these techniques. Detecting diabetic retinopathy illnesses such as exudates, retinal hemorrhage, and micro-aneurysms requires spatial information regarding retinal imaging. The BCSPNFCM (i.e., “Bias Corrected Separated Possibilistic Neighborhood FCM”) algorithm must be introduced for this purpose. BCSPNFCM is [39]:



$$\begin{aligned}
 J_{BCSPNFCM}(U, T, V) &= \sum_{i=1}^c \sum_{j=1}^p (au_{ij}^m D_{ij} + bt_{ij}^n D_{ij}) + \sum_{i=1}^c \sum_{j=1}^p (au_{ij}^m \gamma_i + bt_{ij}^n \gamma_i) \frac{\alpha}{N_r} \\
 &+ \sum_{i=1}^c \sum_{j=1}^p au_{ij}^m X \left( \sum_{l \in N_c} \sum_{s \in N_k} u_{ls}^m \gamma_i \right) \\
 &+ \sum_{i=1}^c \sum_{j=1}^p bt_{ij}^n \left( \sum_{l \in N_c} \sum_{s \in N_k} u_{ls}^n \right) \gamma_i + \sum_{i=1}^c \eta_i \sum_{j=1}^p (1 - t_{ij})^n
 \end{aligned} \tag{4}$$

Fuzzy and possibilistic membership's update equations are as follows [39]:

$$u_{ij} = \sum_{k=1}^c \left( \frac{D_{ij + \frac{\alpha \gamma_i}{N_r} + \sum_{l \in N_c} \sum_{s \in N_k} u_{ls}^m \gamma_i}}{D_{kj + \frac{\alpha}{N_r} + \sum_{l \in N_c} \sum_{s \in N_k} u_{ls}^m \gamma_k}} \right)^{\frac{1}{m-1}} \tag{5}$$

$$t_{ij} = \left( 1 + \frac{b}{\eta_i} \left( D_{ij + \frac{\alpha}{N_r} \gamma_i + \sum_{l \in N_c} \sum_{s \in N_k} t_{ls}^n \gamma_i} \right) \right)^{-\frac{1}{n-1}} \tag{6}$$

The cluster prototype's update equation has been determined to be,

$$v_i = C + D$$

where

$$\begin{aligned}
 C = & \frac{\sum_{j=1}^p (au_{ij}^m y_j + bt_{ij}^n y_j)(au_{ij}^m \beta_j + bt_{ij}^n \beta_j) + \sum_{j=1}^p au_{ij}^m \left( \sum_{l \in N_c} \sum_{s \in N_k} u_{ls}^m \right) \left( \sum_{r \in N_k} (y_r - \beta_r) \right)}{(1 + \alpha) \sum_{j=1}^p (au_{ij}^m + bt_{ij}^n) + \sum_{j=1}^p au_{ij}^m \left( \sum_{l \in N_c} \sum_{s \in N_k} u_{ls}^m \right) + \sum_{j=1}^p bt_{ij}^n \left( \sum_{l \in N_c} \sum_{s \in N_k} t_{ls}^n \right)}
 \end{aligned} \tag{7}$$

$$D =$$

$$\begin{aligned}
 & \frac{\sum_{j=1}^p \frac{\alpha}{N_r} (au_{ij}^m + bt_{ij}^n) \left( \sum_{r \in N_k} (y_r - \beta_r) \right) + \sum_{j=1}^p bt_{ij}^n \left( \sum_{l \in N_c} \sum_{s \in N_k} t_{ls}^n \right) \left( \sum_{r \in N_k} (y_r - \beta_r) \right)}{(1 + \alpha) \sum_{j=1}^p (au_{ij}^m + bt_{ij}^n) + \sum_{j=1}^p au_{ij}^m \left( \sum_{l \in N_c} \sum_{s \in N_k} u_{ls}^m \right) + \sum_{j=1}^p bt_{ij}^n \left( \sum_{l \in N_c} \sum_{s \in N_k} t_{ls}^n \right)}
 \end{aligned}$$

As shown in Figure 9, the suggested blood vessel segmentation algorithm is based on a series of parallel and sequential phases. An example of the proposed blood vessel segmentation results is shown in Figure 10.

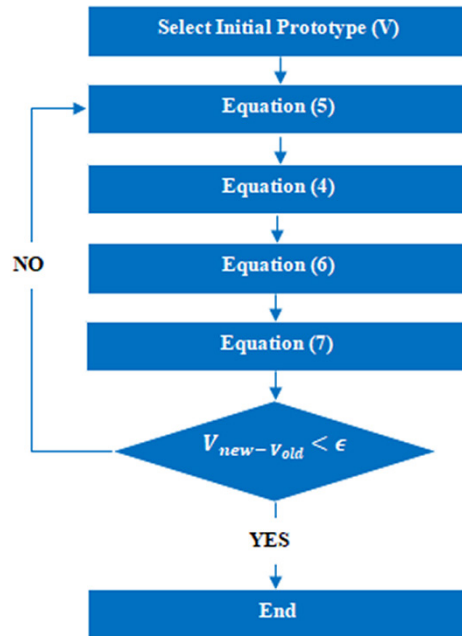


Fig. 9. Block diagram of the proposed blood vessel segmentation algorithm

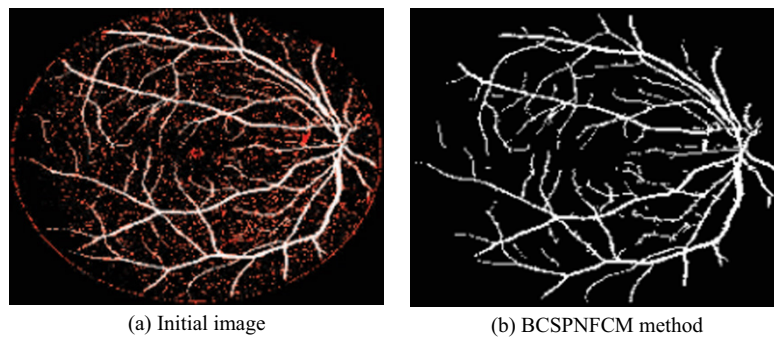


Fig. 10. Blood vessels segmentation

Hemorrhage disease detection and exudates clearance are frequently performed using a blood vessel removal procedure. The first step in removing blood vessels is to use contour detection. The blood vessels are cut out using an edge detection method. Because of the fuzzy enhancing method, the edge detection is the most common strategy to identifying major discontinuities in intensity levels [40]. The IF-THEN rules are the foundation of the fuzzy improvement method [41]. As demonstrated in Figure 11, the edge can be recognized to remove blood vessels.

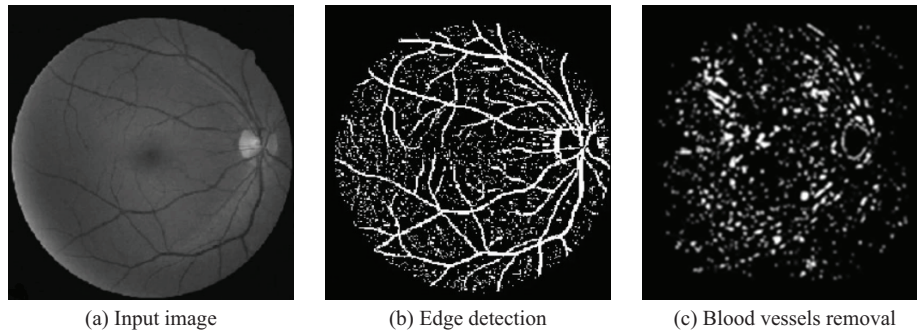


Fig. 11. Blood vessel removal

### 3.4 Elimination-based fovea

Detecting retinal hemorrhages relies heavily on the removal of the fovea. For the most part, the color of the fovea is connected with hemorrhage, but the regions are distinct [42]. To accomplish this, we must remove the fovea. Morphology dilation is the first step in determining the location of the fovea center. It is necessary to perform a dilation operation on a binary image that has a center point known as the fovea center. The fovea has circular properties and a similar size to the dilation structuring element, which has a radius of 25 pixels. To avoid dilation masking of the fovea region, this fovea can be deleted [42]. An example of the fovea elimination results is shown in Figure 12.

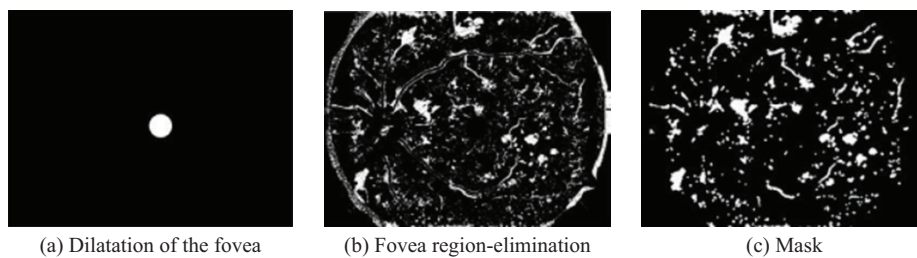


Fig. 12. Elimination-based fovea

### 3.5 Features-based extraction

To accurately describe or diagnose the diabetic retinopathy diseases, we need to extract specific features from retinal Fundus images. Exudates feature extraction, retinal hemorrhage feature extraction, and micro-aneurysms feature extractions are the three characteristics that are extracted in this study. One of the most common complications of diabetes is a hemorrhage in one's own retina. When blood is leaking from the capillaries, they are more vulnerable to harm. Based on splat properties and texture features, a retinal hemorrhage can be identified quickly and easily. To detect retinal hemorrhage,

we use a SVM (i.e., “support vector machine”) in our classification. The following formula is also used to extract textural features [39, 43].

$$Homogeneity_{d,\theta} = \sum_{i=1}^p \sum_{j=1}^p \frac{Pd,\theta}{1+|i-j|} \tag{8}$$

Another complication of diabetes is the yellow flecks of serous leaking from damaged capillaries, as depicted in Figure 2. Between the temporal vascular arcades of the eyes, a golden fleck can be seen, occasionally in a characteristic circular pattern (i.e. clear edge). As a result, exudate characteristics are retrieved at the pixel level [39]. Exudate detection rates based on our research show a high level of accuracy compared to other methods, such as a golden fleck (i.e. retinal hemorrhage, micro-aneurysms, and exudates). Finding exudate characteristics in Fundus images can be done in a variety of ways. Artificial neural network, threshold and morphological approaches are all examples of these methods. Abbadi et al. [44] describes and implements all three approaches. There are two types of blood vessels that can develop micro-aneurysms, the smaller of which allows blood to seep into the capillaries, and the larger of which is more common. Micro-aneurysms (red patches on capillaries) are a common symptom. Diabetic retinopathy is a prevalent cause of micro-aneurysms. Because of this, the correlation co-efficient, shape, gray-scale, color intensity, and pixel intensity presented and implemented in [45] are effective for extracting micro-aneurysms’ characteristics.

### 3.6 Features-based selection and classification

As a general rule, feature selection is used to limit the amount of characteristics by focusing on the most important ones. Typically, feature selection is used for two purposes: to reduce the quantity of the vocabulary input and to improve the accuracy of predictions. Retinal hemorrhage, exudates, and micro-aneurysm have been retrieved in this paper, and the appropriate characteristics have been picked using the DCNN (“Deep Convolutional Neural Network”) as implemented and discussed in [46, 47]. The retinal Fundus images are classified by a DCNN shown in Figure 13.

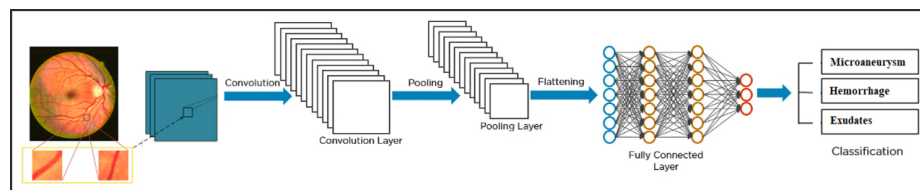
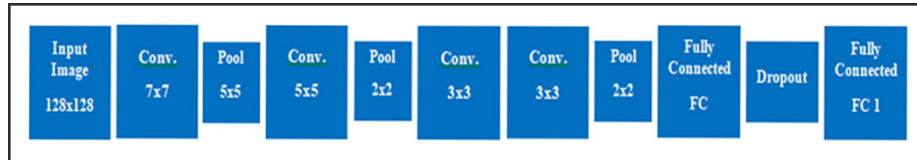


Fig. 13. DCNN architecture

The DCNN architecture consists of four convolutional layers and two fully-connected layers. Third convolution layer is fed straight from the third convolution layer after contrast normalization, pooling, and a non-linear function are applied. After being molded into a feature vector, the output of the convolution layer is passed to the fully-connected layers for the purpose of classification. Figure 14 shows the architectural details.



**Fig. 14.** DCNN Architecture (Conv. = Convolution; Pool = Pooling; FC = Fully Connected)

Table 2 depicts the parameters of the described layers. The 40 epochs of training were scrambled so that each epoch had a new set of data. Use of a 10 GB NVIDIA Ge-Force 2080 TI graphics card was used to train for the proposed approach.

**Table 2.** DCNN architecture-parameters

Layer	Output Size	Kernal Size	Stride	No. of Kernels
Input	128×128	–	–	–
Convolutional	122×122×32	7×7	1	32
Max-Pooling	61×61×32	2×2	2	–
Convolutional	57×57×64	5×5	1	64
Max-Pooling	28×28×64	2×2	2	–
Convolutional	26×26×128	3×3	1	128
Convolutional	24×24×256	3×3	1	256
Max-Pooling	12×12×256	2×2	2	–
Full-Connected	4096	–	–	–
Full-Connected	2 Classes	–	–	–

## 4 Experimental analysis and evaluation

This section mostly focuses on evaluating the suggested algorithm’s performance. Segmentation and classification are used in the proposed diabetic retinopathy detection and categorization of retinal disease. CPFC Mused for blood vessel segmentation (Constrained Possibilistic Fuzzy C-Means). To improve sensitivity and precision, diabetic retinopathy illnesses should be classified using SVMGA classifications. We’ve compared our BCSPNFCM segmentation algorithm to current state-of-the-art algorithms. SVMGA was compared to some earlier classifiers for classification purposes. As demonstrated in Figure 15, phase-by-phase findings of the proposed approach.

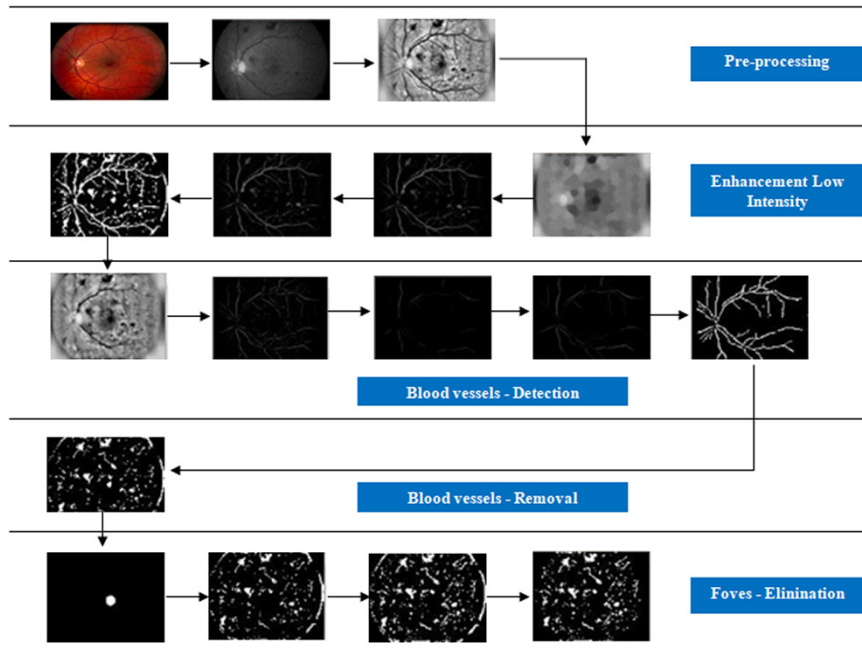


Fig. 15. Phase-by-phase findings of the proposed approach

#### 4.1 Dataset

Diabetic retinopathy can be detected using the Kaggle dataset, which is well-known and widely utilized. There are 88,702 retinal Fundus images in this dataset in total. Eye-PACS created a Kaggle dataset for free in order to help researchers. 35,126 Fundus images were used for practice (i.e., training) and 53,576 for testing in this collection. A list of datasets for research into diabetic retinopathy is provided in Table 3 [48, 49].

Table 3. Datasets for diabetic retinopathy

Dataset – Name	Availability – Online	Usage Rate – Citation	No. of Images – In Total
Kaggle	Available	76%	88702
DIARETDB1	Available	82%	89
DIARETDB0	Available	20%	130
STARE	Available	26%	400
DRIVE	Available	26%	40
Messidor-2	Available	3%	1748
Messidor	Available	43%	1200
FAZ	Available	3%	60
E-Ophtha	Available	30%	381
ROC	Available	23%	100

(Continued)

**Table 3.** Datasets for diabetic retinopathy (Continued)

Dataset – Name	Availability – Online	Usage Rate – Citation	No. of Images – In Total
DR1	Available	3%	234
DR2	Available	6%	520
DRiDB	Available	10%	50
JMU	Not-available	3%	85
TMUMDH	Not-available	3%	414
Moorfield	Not-available	3%	21536
KMCN. India	Not-available	3%	122

#### 4.2 Performance evaluation

The purpose of this study is to offer new image processing approaches for detecting retinal disease, using retinal Fundus images. It is in this section that the evaluation of performance measures is presented. Metrics evaluation and analysis were undertaken to assess the effectiveness of the proposed strategy. Many studies begin with a comparison of the performance of several algorithms. Because of this, we have compared the suggested method’s findings to those of existing methods. The most commonly employed measures include, for example (i.e. accuracy, specificity, and sensitivity). There are three distinct sets of performance measurements are given by [40, 50]:

$$Accuracy = \frac{TN + TP}{TN + TP + FN + FP} \tag{9}$$

$$Specificity = \frac{TN}{TN + FP} \tag{10}$$

$$Sensitivity = \frac{TP}{TP + FN} \tag{11}$$

For each step, we’ve employed a different algorithm in our new approach. Diabetic retinopathy disease can be identified using any of these approaches. A series of procedures, depicted in Figure 14, is required to achieve this goal. We must enhance our sensitivity and specificity in order to meet these requirements. Then, improve classification and segmentation accuracy as well. Figure 6 shows the results of CLAHE (“Contrast Limited Adaptive Histogram Equalization”). A segmentation procedure for the blood vessels, Figure 10 shows that BCSPNFCM can produce results as efficient as those displayed in the figure. Based on our performance data, we should compare our segmentation accuracy to [40]. Segmentation performance should be compared in Table 4. Figure 11 depicts the removal of blood vessels using fuzzy based edge enhancement. Thus, a clean section of the deleted portion will be produced. We were able to accurately identify diabetic retinopathy diseases using feature extraction based on all features. Features should be reduced by employing an un-supervised learning technique for feature selection. SVMGA, rather than SVM plus PNN, should be used

for classification because it is more efficient and effective. Accuracy, specificity, and sensitivity should all improve. Comparability results are shown in Table 5.

**Table 4.** Accuracy of segmentation-based comparison

Method	Accuracy
BCSPNFCM	98.438
Watershed Transform	95.783
Automatic Thresholding	69.300
Atlas Based	96.827
ICDT	86.400
Graph Cut	97.588

**Table 5.** Performance metric evaluation – comparison

Method	Sensitivity	Specificity	Accuracy
Proposed-SVMGA	99.20	96.40	98.80
MSR-net	97.00	82.00	98.30
SVM	98.71	96.07	97.60
PSO-GIT2FMS	98.4	96.00	96.66
PNN	90.86	88.02	89.60
CNN	98.71	96.04	97.54

Moreover, as depicted in Figure 16, the AUC curve comparison of the proposed approach. Each method’s outcome was represented graphically by a curve. As compared to previous approaches, this one has a greater area under the curve at 98.8 percent True positive and false positive values are placed side by side on the graph to illustrate this.

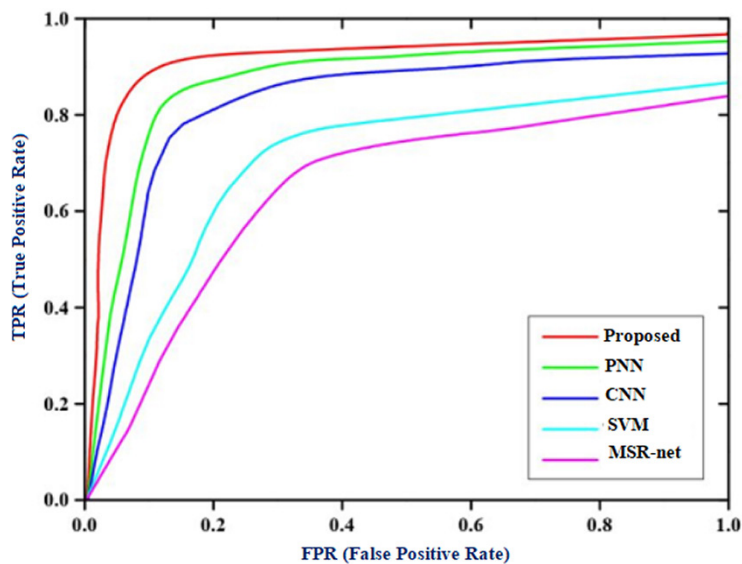


**Fig. 16.** AUC curve – comparisons



Interestingly, the effectiveness of contemporary healthcare services, such as computerized diagnosis and individualized therapy, relies heavily on the availability of datasets. The size of the dataset is regarded as a crucial factor in determining the performance of a machine learning model. Large datasets typically result in improved classification performance, whereas short datasets may result in over-fitting [51]. Table 6 details the effect of training dataset size on the proposed approach’s performance (i.e., accuracy).

**Table 6.** The impact of training dataset size on the performance of the proposed approach

Dataset – Name	Dataset – Size	Performance of the Proposed Approach – Accuracy
Kaggle	88702	98.80
Messidor-2	1748	98.63
Messidor	1200	98.59
STARE	400	98.45
DIARETDB0	130	98.37
DIARETDB1	89	98.30
DRIVE	40	98.21

## 5 Conclusion

A new approach for detecting diabetic retinopathy using retinal Fundus images based on a combination of image processing and artificial intelligence has been proposed in this research. Diabetic retinopathy features extraction and feature classification were the two phases of the proposed image processing approach. The new image processing approach had a number of interesting qualities. Diabetes retinopathy detection has been developed and implemented in a number of stages. To ensure the accuracy of the results, the ophthalmologists compared the MATLAB simulation results to those of the experts. The test results demonstrate that the sensitivity, specificity, and accuracy are above 99.20%, 96.40% and 98.80 respectively were all quite successful in comparison to other state-of-the-art approaches.

## 6 References

- [1] S. K. Saha, D. Xiao, A. Bhuiyan, T. Y. Wong, and Y. Kanagasigam, “Color fundus image registration techniques and applications for automated analysis of diabetic retinopathy progression: A review,” *Biomedical Signal Processing and Control*, vol. 47, pp. 288–302, 2019. <https://doi.org/10.1016/j.bspc.2018.08.034>
- [2] N. Gharaibeh, O. M. Al-Hazaimeh, B. Al-Naami, and K. M. Nahar, “An effective image processing method for detection of diabetic retinopathy diseases from retinal fundus images,” *International Journal of Signal and Imaging Systems Engineering*, vol. 11, pp. 206–216, 2018. <https://doi.org/10.1504/IJSISE.2018.093825>
- [3] N. Gharaibeh, O. M. Al-hazaimeh, A. Abu-Ein, and K. M. Nahar, “A hybrid SVM Naïve-Bayes classifier for bright lesions recognition in eye fundus images,” *International Journal on Electrical Engineering and Informatics*, vol. 13, pp. 530–545, 2021. <https://doi.org/10.15676/ijeeci.2021.13.3.2>

- [4] S. H. Abbood, H. N. Abdull Hamed, M. S. Mohd Rahim, A. H. M. Alaidi, and H. T. Salim ALRikabi, "DR-LL Gan: Diabetic retinopathy lesions synthesis using generative adversarial network," *International Journal of Online & Biomedical Engineering*, vol. 18, 2022. <https://doi.org/10.3991/ijoe.v18i03.28005>
- [5] S. Joshi and P. Karule, "A review on exudates detection methods for diabetic retinopathy," *Biomedicine & Pharmacotherapy*, vol. 97, pp. 1454–1460, 2018. <https://doi.org/10.1016/j.biopha.2017.11.009>
- [6] R. Pires, S. Avila, J. Wainer, E. Valle, M. D. Abramoff, and A. Rocha, "A data-driven approach to referable diabetic retinopathy detection," *Artificial Intelligence In Medicine*, vol. 96, pp. 93–106, 2019. <https://doi.org/10.1016/j.artmed.2019.03.009>
- [7] S. K. Raju Maher and D. M. Dhopeswarkar, "Review of automated detection for diabetes retinopathy using fundus images," *International Journal of Advanced Research in Computer Science and Software Engineering*, vol. 5, 2015.
- [8] K. Verma, P. Deep, and A. Ramakrishnan, "Detection and classification of diabetic retinopathy using retinal images," in *2011 Annual IEEE India Conference*, 2011, pp. 1–6. <https://doi.org/10.1109/INDCON.2011.6139346>
- [9] K. Wisaeng, N. Hiransakolwong, and E. Pothiruk, "Automatic detection of exudates in diabetic retinopathy images," *Journal of Computer Science*, vol. 8, p. 1304, 2012. <https://doi.org/10.3844/jcssp.2012.1304.1313>
- [10] M. P. Paing, S. Choomchuay, and M. R. Yodprom, "Detection of lesions and classification of diabetic retinopathy using fundus images," in *2016 9th Biomedical Engineering International Conference (BMEiCON)*, 2016, pp. 1–5. <https://doi.org/10.1109/BMEiCON.2016.7859642>
- [11] M. Purandare and K. Noronha, "Hybrid system for automatic classification of diabetic retinopathy using fundus images," in *2016 Online International Conference on Green Engineering and Technologies (IC-GET)*, 2016, pp. 1–5. <https://doi.org/10.1109/GET.2016.7916623>
- [12] L. Zhou, Y. Zhao, J. Yang, Q. Yu, and X. Xu, "Deep multiple instance learning for automatic detection of diabetic retinopathy in retinal images," *IET Image Processing*, vol. 12, pp. 563–571, 2018. <https://doi.org/10.1049/iet-ipr.2017.0636>
- [13] S. Suriyal, C. Druzgalski, and K. Gautam, "Mobile assisted diabetic retinopathy detection using deep neural network," in *2018 Global Medical Engineering Physics Exchanges/ Pan American Health Care Exchanges (GMEPE/PAHCE)*, pp. 1–4, 2018. <https://doi.org/10.1109/GMEPE-PAHCE.2018.8400760>
- [14] V. Gulshan, L. Peng, M. Coram, M. C. Stumpe, D. Wu, A. Narayanaswamy, et al., "Development and validation of a deep learning algorithm for detection of diabetic retinopathy in retinal fundus photographs," *Jama*, vol. 316, pp. 2402–2410, 2016. <https://doi.org/10.1001/jama.2016.17216>
- [15] W. M. Gondal, J. M. Köhler, R. Grzeszick, G. A. Fink, and M. Hirsch, "Weakly-supervised localization of diabetic retinopathy lesions in retinal fundus images," in *2017 IEEE International Conference on Image Processing (ICIP)*, pp. 2069–2073, 2017. <https://doi.org/10.1109/ICIP.2017.8296646>
- [16] O. Faust, R. Acharya U, E. Y.-K. Ng, K.-H. Ng, and J. S. Suri, "Algorithms for the automated detection of diabetic retinopathy using digital fundus images: A review," *Journal of Medical Systems*, vol. 36, pp. 145–157, 2012. <https://doi.org/10.1007/s10916-010-9454-7>
- [17] P. Khojasteh, L. A. P. Júnior, T. Carvalho, E. Rezende, B. Aliahmad, J. P. Papa, et al., "Exudate detection in fundus images using deeply-learnable features," *Computers in Biology and Medicine*, vol. 104, pp. 62–69, 2019. <https://doi.org/10.1016/j.compbiomed.2018.10.031>
- [18] A. R. Chowdhury, T. Chatterjee, and S. Banerjee, "A random forest classifier-based approach in the detection of abnormalities in the retina," *Medical & Biological Engineering & Computing*, vol. 57, pp. 193–203, 2019. <https://doi.org/10.1007/s11517-018-1878-0>

- [19] J. Kaur and D. Mittal, "A generalized method for the segmentation of exudates from pathological retinal fundus images," *Biocybernetics and Biomedical Engineering*, vol. 38, pp. 27–53, 2018. <https://doi.org/10.1016/j.bbe.2017.10.003>
- [20] A. Kwasigroch, B. Jarzembinski, and M. Grochowski, "Deep CNN based decision support system for detection and assessing the stage of diabetic retinopathy," in *2018 International Interdisciplinary PhD Workshop (IIPHDW)*, 2018, pp. 111–116. <https://doi.org/10.1109/IIPHDW.2018.8388337>
- [21] R. Tennakoon, D. Mahapatra, P. Roy, S. Sedai, and R. Garnavi, "Image quality classification for DR screening using convolutional neural networks," *Proceedings of the 2016 Ophthalmic*, 2016. <https://doi.org/10.17077/omia.1054>
- [22] M. Omar, F. Khelifi, and M. A. Tahir, "Detection and classification of retinal fundus images exudates using region based multiscale LBP texture approach," in *2016 International Conference on Control, Decision and Information Technologies (CoDIT)*, 2016, pp. 227–232. <https://doi.org/10.1109/CoDIT.2016.7593565>
- [23] S. S. Rahim, V. Palade, J. Shuttleworth, and C. Jayne, "Automatic screening and classification of diabetic retinopathy and maculopathy using fuzzy image processing," *Brain Informatics*, vol. 3, pp. 249–267, 2016. <https://doi.org/10.1007/s40708-016-0045-3>
- [24] K. Adem, M. Hekim, and S. Demir, "Detection of hemorrhage in retinal images using linear classifiers and iterative thresholding approaches based on firefly and particle swarm optimization algorithms," *Turkish Journal of Electrical Engineering & Computer Sciences*, vol. 27, pp. 499–515, 2019. <https://doi.org/10.3906/elk-1804-147>
- [25] J. Wu, S. Zhang, Z. Xiao, F. Zhang, L. Geng, S. Lou, et al., "Hemorrhage detection in fundus image based on 2D Gaussian fitting and human visual characteristics," *Optics & Laser Technology*, vol. 110, pp. 69–77, 2019. <https://doi.org/10.1016/j.optlastec.2018.07.049>
- [26] L. Guo, J.-J. Yang, L. Peng, J. Li, and Q. Liang, "A computer-aided healthcare system for cataract classification and grading based on fundus image analysis," *Computers in Industry*, vol. 69, pp. 72–80, 2015. <https://doi.org/10.1016/j.compind.2014.09.005>
- [27] D. K. Prasad, L. Vibha, and K. Venugopal, "Early detection of diabetic retinopathy from digital retinal fundus images," in *2015 IEEE Recent Advances in Intelligent Computational Systems (RAICS)*, 2015, pp. 240–245. <https://doi.org/10.1109/RAICS.2015.7488421>
- [28] M. Mateen, J. Wen, S. Song, and Z. Huang, "Fundus image classification using VGG-19 architecture with PCA and SVD," *Symmetry*, vol. 11, p. 1, 2018. <https://doi.org/10.3390/sym11010001>
- [29] L. Wu, C. Wan, Y. Wu, and J. Liu, "Generative caption for diabetic retinopathy images," in *2017 International Conference on Security, Pattern Analysis, and Cybernetics (SPAC)*, 2017, pp. 515–519. <https://doi.org/10.1109/SPAC.2017.8304332>
- [30] H. Zhao, H. Li, S. Maurer-Stroh, Y. Guo, Q. Deng, and L. Cheng, "Supervised segmentation of un-annotated retinal fundus images by synthesis," *IEEE Transactions on Medical Imaging*, vol. 38, pp. 46–56, 2018. <https://doi.org/10.1109/TMI.2018.2854886>
- [31] S. H. Bhat and P. Kumar, "Segmentation of optic disc by localized active contour model in retinal fundus image," in *Smart Innovations in Communication and Computational Sciences*, ed: Springer, 2019, pp. 35–44. [https://doi.org/10.1007/978-981-13-2414-7\\_4](https://doi.org/10.1007/978-981-13-2414-7_4)
- [32] M. S. Miri, M. D. Abramoff, K. Lee, M. Niemeijer, J.-K. Wang, Y. H. Kwon, et al., "Multimodal segmentation of optic disc and cup from SD-OCT and color fundus photographs using a machine-learning graph-based approach," *IEEE Transactions on Medical Imaging*, vol. 34, pp. 1854–1866, 2015. <https://doi.org/10.1109/TMI.2015.2412881>
- [33] N.-M. Tan, Y. Xu, W. B. Goh, and J. Liu, "Robust multi-scale superpixel classification for optic cup localization," *Computerized Medical Imaging and Graphics*, vol. 40, pp. 182–193, 2015. <https://doi.org/10.1016/j.compmedimag.2014.10.002>

- [34] O. M. Al-Hazaimeh, "Combining audio samples and image frames for enhancing video security," *Indian Journal of Science and Technology*, vol. 8, p. 940, 2015. <https://doi.org/10.17485/ijst/2015/v8i10/53149>
- [35] J. Ma, X. Fan, S. X. Yang, X. Zhang, and X. Zhu, "Contrast limited adaptive histogram equalization-based fusion in YIQ and HSI color spaces for underwater image enhancement," *International Journal of Pattern Recognition and Artificial Intelligence*, vol. 32, p. 1854018, 2018. <https://doi.org/10.1142/S0218001418540186>
- [36] M. Al-Nawashi, O. M. Al-Hazaimeh, and M. Saraee, "A novel framework for intelligent surveillance system based on abnormal human activity detection in academic environments," *Neural Computing and Applications*, vol. 28, pp. 565–572, 2017. <https://doi.org/10.1007/s00521-016-2363-z>
- [37] N. M. Sasi and V. Jayasree, "Contrast limited adaptive histogram equalization for qualitative enhancement of myocardial perfusion images," *Engineering*, vol. 5, pp. 326–331, 2013. <https://doi.org/10.4236/eng.2013.510B066>
- [38] R. R. Sariha, V. Paul, and P. G. Kumar, "Content based image retrieval using deep learning process," *Cluster Computing*, vol. 22, pp. 4187–4200, 2019. <https://doi.org/10.1007/s10586-018-1731-0>
- [39] J. Aparajeeta, P. K. Nanda, and N. Das, "Modified possibilistic fuzzy C-means algorithms for segmentation of magnetic resonance image," *Applied Soft Computing*, vol. 41, pp. 104–119, 2016. <https://doi.org/10.1016/j.asoc.2015.12.003>
- [40] A. U. R. Khan and K. Thakur, "An efficient fuzzy logic based edge detection algorithm for gray scale image," 2012.
- [41] S. Sarangi, S. K. Sabut, and D. Majhi, "Evaluation and comparison of retinal blood vessels extraction using edge detectors in diabetic retinopathy," *International Journal of Signal and Imaging Systems Engineering*, vol. 9, pp. 174–183, 2016. <https://doi.org/10.1504/IJSISE.2016.076229>
- [42] S. Bortolin and D. Welfer, "Automatic detection of microaneurysms and hemorrhages in color eye fundus images," *AIRCC's International Journal of Computer Science and Information Technology*, vol. 5, pp. 21–37, 2013. <https://doi.org/10.5121/ijcsit.2013.5502>
- [43] O. M. Al-Hazaimeh, M. Al-Nawashi, and M. Saraee, "Geometrical-based approach for robust human image detection," *Multimedia Tools and Applications*, vol. 78, pp. 7029–7053, 2019. <https://doi.org/10.1007/s11042-018-6401-y>
- [44] N. K. El Abbadi and E. H. Al-Saadi, "Automatic detection of exudates in retinal images," *International Journal of Computer Science Issues (IJCSI)*, vol. 10, p. 237, 2013.
- [45] N. Y. Gharaibeh, "A novel approach for detection of microaneurysms in diabetic retinopathy disease from retinal fundus images," *Comput. Inf. Sci.*, vol. 10, pp. 1–15, 2017. <https://doi.org/10.5539/cis.v10n1p1>
- [46] Y. Sun, B. Xue, M. Zhang, G. G. Yen, and J. Lv, "Automatically designing CNN architectures using the genetic algorithm for image classification," *IEEE Transactions on Cybernetics*, vol. 50, pp. 3840–3854, 2020. <https://doi.org/10.1109/TCYB.2020.2983860>
- [47] O. M. Al-Hazaimeh and M. Al-Smadi, "Automated pedestrian recognition based on deep convolutional neural networks," *International Journal of Machine Learning and Computing*, vol. 9, pp. 662–667, 2019. <https://doi.org/10.18178/ijmlc.2019.9.5.855>
- [48] M. Mateen, J. Wen, M. Hassan, N. Nasrullah, S. Sun, and S. Hayat, "Automatic detection of diabetic retinopathy: A review on datasets, methods and evaluation metrics," *IEEE Access*, vol. 8, pp. 48784–48811, 2020. <https://doi.org/10.1109/ACCESS.2020.2980055>
- [49] M. Siddique, A. Aziz, J. Ferdouse, M. Habib, M. Mia, and M. S. Uddin, "Convolutional neural network modeling for eye disease recognition," *International Journal of Online & Biomedical Engineering*, vol. 18, 2022. <https://doi.org/10.3991/ijoe.v18i09.29847>

- [50] V. T. H. Tuyet, N. T. Binh, and D. T. Tin, “A deep bottleneck U-Net combined with saliency map for classifying diabetic retinopathy in fundus images,” *International Journal of Online & Biomedical Engineering*, vol. 18, 2022. <https://doi.org/10.3991/ijoe.v18i02.27605>
- [51] A. Althnian, D. AlSaeed, H. Al-Baity, A. Samha, A. B. Dris, N. Alzakari, et al., “Impact of dataset size on classification performance: An empirical evaluation in the medical domain,” *Applied Sciences*, vol. 11, p. 796, 2021. <https://doi.org/10.3390/app11020796>

## 7 Authors

**Obaida M. Al-Hazaimeh** earned a BSc in Computer Science from Jordan’s Applied Science University in 2004 and an MSc in Computer Science from Malaysia’s University Science Malaysia in 2006. In 2010, he earned a PhD in Network Security (Cryptography) from Malaysia. He is an Full professor at Al-Balqa Applied University’s Department of Computer Science and Information Technology. Cryptology, image processing, machine learning, and chaos theory are among his primary research interests. He has published around 45 papers in international refereed publications as an author or co-author. He can be contacted at email: [dr\\_obaida@bau.edu.jo](mailto:dr_obaida@bau.edu.jo).

**Ashraf A. Abu-Ein** is an Associate Professor in the Department of Electrical Engineering. He has completed his PhD at National Technical University of Ukraine, Computer Engineering. “Computers, Computing Systems and Networks”, 2007. Now, he is a lecturer at Al-Balqa Applied University–Al-huson University College, Jordan. He can be contacted at email: [ashraf.abuain@bau.edu.jo](mailto:ashraf.abuain@bau.edu.jo).

**Nedal M. Tahat** received his BSc in Mathematics at the Yarmouk University, Jordan, in 1994, and MSc in Pure Mathematics at Al al-Bayt University, Jordan, in 1998. He is a PhD candidate in Applied Number Theory (Cryptography) from the National University of Malaysia (UKM), in 2010. He is an Full Professor at the Department Mathematics, Hashemite University. His main research interests are cryptology and number theory. He has published more than 50 papers, authored/co-authored, and more than 15 refereed journal and conference papers. He can be contacted at email: [nedal@hu.edu.jo](mailto:nedal@hu.edu.jo).

**Ma’moun A. Al-Smadi** is an Lecturer in the Department of Electrical Engineering. at Al-Balqa Applied University, Al-Huson University College, Jordan. He has completed his PhD at Universiti Sains Islam Malaysia in 2021. His main research interests are image processing and machine learning. He can be contacted at email: [ma\\_smadi@bau.edu.jo](mailto:ma_smadi@bau.edu.jo).

**Malek M. Al-Nawashi** is an a Lecturer in the Department of Computer Science and Information Technology at Al-Balqa Applied University–Al-huson University College, Jordan. He has completed his PhD at University of Salford Manchester in Computer Science in 2019. His main research interests are image processing and machine learning. He can be contacted at email: [nawashi@bau.edu.jo](mailto:nawashi@bau.edu.jo).

Article submitted 2022-07-13. Resubmitted 2022-08-13. Final acceptance 2022-08-19. Final version published as submitted by the authors.